ORGANOMETALLICS

Article

pubs.acs.org/Organometallics

Photocatalytic Carbon−Carbon σ-Bond Anaerobic Oxidation of Ketones with Water by Rhodium(III) Porphyrins

Siu Yin Lee and Kin Shing Chan*

Department of Chemistry, The Chinese University of Hong Kong, Shatin, New Territories, Hong Kong, People's Republic of China

Supporting Information

ABSTRACT: Photocatalytic carbon−carbon σ-bond oxidation of unstrained ketones by water using rhodium(III) porphyrin catalyst was accomplished. The catalysis yielded the corresponding one-carbon-less carbonyl compound and H_2 with up to 30 turnovers in both aliphatic and cyclic ketones with α substituents. No carbon loss was observed in aromatic ketone. Mechanistic studies suggest that $(Ph_3P)Rh^{III}(ttp)OH$ (ttp = tetratolylporphyrinato dianion) is the key intermediate in the carbon−carbon σ-bond anaerobic oxidation.

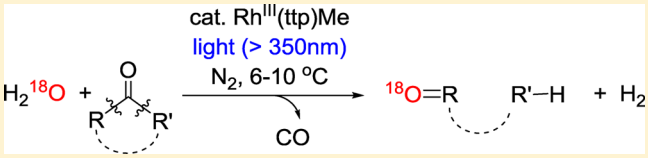

INTRODUCTION

Catalytic cleavage of carbon−carbon σ bonds has recently been accentuated in organometallic research,[1] since it has emerged as an important strategy for structural modification in synthetic chemistry.[2] However, catalytic carbon−carbon bond activation (CCA) is kinetically very challenging, as carbon−hydrogen bond activation (CHA) is usually a more competitive process,[3] as a result of the more abundant and more easily accessible C−H bonds in hydrocarbons.[4] With the aid of the robust metalloporphyrins that can endure high temperatures, certain stoichiometric selective CCA under thermal conditions have been developed over the past decade.[5−7]

Despite the success in stoichiometric reactions, catalytic functionalization strategies thus far are quite limited. Murakami and Ito et al.[8] developed the strain-released CCA of cyclobutanone derivatives catalyzed by rhodium(I). Suggs[9] and Jun et al.[9,10] discovered the CCA of acylquinolines assisted by the chelation of substrate on the rhodium catalyst. Chatani et al.[11] also reported the decarbonylative CCA in aromatic ketones bearing an oxazoline or pyridine as the chelating group on ruthenium. Other catalytic CCA examples include the catalytic hydrogenation of $C(sp^2)−C(sp^2)$ bonds in biaryls, as illustrated by Jones et al.,[12] and the rhodium-catalyzed $C(sp^2)−C(sp^3)$ bond hydrogenation or hydrosilylation of diphosphine mesitylene derivatives documented by Milstein et al.[13] The catalytic $C(sp^3)−C(sp^3)$ bond hydrogenation of [2.2]-paracyclophane was also recently reported by the Chan group.[14] In addition to these remarkable advances, mild and selective catalytic CCA on nonstrained substrates remains rare.

The Chan group has reported the stoichiometric CCA of 2,6-dimethylcyclohexanone by $Rh^{III}(ttp)Me$ to give $Rh^{III}(ttp)-COCHMe(CH_2)_3COMe$ (eq 1).[15] The water-promoted CCA of ketone suggests that $Rh^{III}(ttp)OH$ generated from the hydrolysis of $Rh^{III}(ttp)Me$ is the proposed key intermediate in the CCA step, in accordance with the reaction stoichiometry. However, as the strong Rh−C(CO) bond (54 kcal mol^{-1})[16] remains intact even at the high temperature of 200 °C in the presence of H_2O, the high stability limits further development in thermal catalysis.[15]

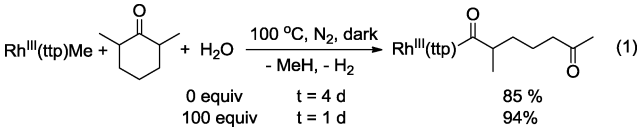

To further functionalize the thermally and hydrolytically stable Rh−C(CO) bond, we took advantage of the known homolytic cleavage of (tmp)Rh−Me (tmp = tetramesitylporphyrinato dianion) to generate $Rh^{II}(tmp)$ through photolysis.[17] Photolysis at $\lambda > 350$ nm provides extra energy up to 81.6 kcal mol^{-1} to cleave the Rh−C(CO) bond homolytically for further catalytic reaction. Metalloporphyrin-based photocatalysis is a growing area due to the attractive high visible-light absorptivity of metalloporphyrins.[18] Examples include photocatalytic hydrogen generation,[19] photocatalytic dehydrogenation from alcohol,[20] photoreduction of carbon dioxide to carbon monoxide,[21] and photooxidation of phenol[22] and aromatic aldehyde.[23]

Catalytic oxidation of the σ carbon−carbon bond using water is another key focus in this report. Current research on photocatalysis using H_2O as the oxygen source is well exemplified in the hydroxylation of silyl alkane,[24] epoxidation of alkenes,[25−27] and oxidation of alcohols[26−29] and sulfides.[27,29,30]

Herein, we present the photocatalytic oxidation of the stronger and more robust carbon−carbon bond in unstrained ketones using rhodium(III) porphyrin catalysts and water under anaerobic conditions to yield the corresponding oxygen-incorporated organics and H_2 (Scheme 1). H_2O serves as the oxygen source in the one-pot reaction.

Received: July 8, 2013
Published: September 19, 2013

dx.doi.org/10.1021/om400672t | Organometallics 2013, 32, 5391−5401

Scheme 1. Catalytic Carbon−Carbon Bond Oxidation with H_2O

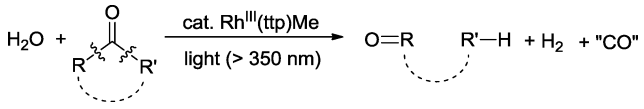

RESULTS AND DISCUSSION

Initially, the light-induced catalytic carbon−carbon σ-bond oxidation of 2,6-dimethylcyclohexanone by Rh^{III}(tmp)Me was achieved under ambient conditions to yield 2-heptanone in 9 turnovers (detected by GC/MS) using a 400 W mercury halide lamp (eq 2).

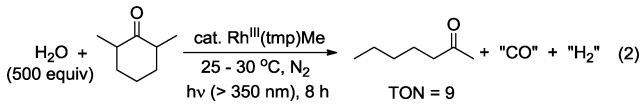

(2)

To improve the catalytic efficiency, the effects of (1) porphyrin ligand, (2) donor ligand loading, (3) temperature, (4) water concentration, and (5) solvent polarity on catalysis were studied independently. The sterically less hindered Rh^{III}(ttp)Me catalyzed the transformation to give higher turnovers than for Rh^{III}(tmp)Me (Table 1, entries 1 and 2). The catalysis was promoted by the addition of PPh_3 (Table 1, entries 2 and 3). This suggests that the phosphine ligand effectively trapped Rh^{III}(ttp)OH to generate a higher effective concentration of $(Ph_3P)Rh^{III}$(ttp)OH at 6−10 °C. Lower temperatures promoted the catalytic activity of Rh^{III}(ttp)Me (Table 1, entries 2, 4, and 5). Presumably, $(Ph_3P)Rh^{III}$(ttp)OH is more stable at lower temperature to account for the improved TONs. Rh^{III}(ttp)OH ((ttp)Rh−OH, 46 kcal mol^{-1})[31] is known to be thermally unstable over 60 °C to give Rh^{II}(ttp) and H_2O_2.[32] A higher loading of water also enhanced the TONs significantly (Table 1, entries 6−8). At higher H_2O concentration, the equilibrium of Rh(II) disproportionation by H_2O would be shifted to maintain a higher concentration of $(Ph_3P)Rh^{III}$(ttp)OH (eq 3),[33] supporting its key role in catalysis. A 350 nm UV filter was applied to eliminate the Norrish type I or II reaction in all of the photolysis reactions.[34] A control experiment was also carried out to confirm the catalytic role of rhodium porphyrins. Without rhodium porphyrins, no catalysis occurred (Table 1, entry 9). After screening through different conditions, the reaction was optimized at 6−10 °C and 500 equiv of H_2O with Rh^{III}(ttp)Me as the catalyst.

(3)

To our delight, the catalysis is also applicable to various ketones under the optimized conditions (Table 2). Photocatalytic CCA of diisopropyl ketone successfully yielded acetone (Table 2, entry 1). However, propane, as expected from the reaction stoichiometry, was not observed due to the detection difficulty of low-molecular-weight compounds. Cyclic ketones were then employed as intramolecular traps. Photocatalytic activation of 2-methylcyclohexanone gave a better yield of 2-hexanone with the selective cleavage of the more hindered but weaker (C=O)−CH(Me)R bond (~81.3 kcal mol^{-1})[35] in comparison to the (C=O)−CH_2R bond (~84.1 kcal mol^{-1})[35] (Table 2, entry 2). 2,6-Dimethylcyclohexanone, with an extra isopropyl moiety, was photolyzed to yield 2-heptanone with a much improved turnover (Table 2, entry 3).

Table 1. Optimization of Photocatalysis

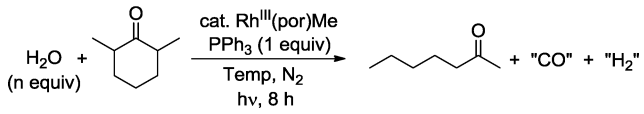

entry[a]	catalyst	temp (°C)	amt of H_2O (equiv)	solvent	TON	TOF (10^{-4} s^{-1})
1	Rh(tmp)Me	25−30	500		12.6	4.4
2	Rh(ttp)Me	25−30	500		21.1	7.3
3[b]	Rh(ttp)Me	25−30	500		11.3	3.9
4	Rh(ttp)Me	50−60	500		15.9	5.5
5	Rh(ttp)Me	6−10	500		29.6	10.3
6	Rh(ttp)Me	6−10	50		7.8	2.7
7	Rh(ttp)Me	6−10	100		9.5	3.3
8	Rh(ttp)Me	6−10	1000		31.0	10.7
9	no catalyst	50−60	500		0	0
10[c]	Rh(ttp)Me	6−10	500	benzene	19.3	6.7
11[c]	Rh(ttp)Me	6−10	500	acetone	18.6	6.5

[a]A 400 W quartz mercury halide lamp was used. A B+W 67 mm MRC UV filter was used for cutting off light rays below 350 nm. [b]No PPh_3 was added. [c]Conditions: 1000 equiv of 2,6-dimethylcyclohexanone, concentration 2.57 M; solvent-free conditions, concentration 7.33 M.

Table 2. Substrate Scope of Photocatalytic CCA by Rh^{III}(ttp)Me

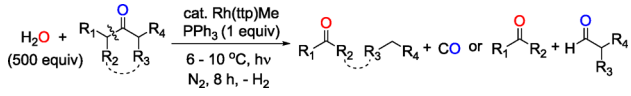

Entry[a]	Ketone	Product	TON	TOF (× 10-4 s-1)
1			8.9	3.1
2		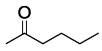	13.9	4.8
3			29.6	10.3
4b	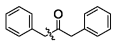	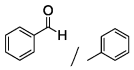	4.9 / 1.3	1.70 / 0.45
5		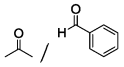	3.9 / 4.9	1.35 / 1.70
6		No Product	0	0

[a]A 400 W quartz mercury halide lamp was used. A B+W 67 mm MRC UV filter was used for cutting off light rays below 350 nm. [b]Reaction temperature 50−60 °C.

dx.doi.org/10.1021/om400672t | Organometallics 2013, 32, 5391−5401

1,3-Diphenylacetone was also photocatalytically activated to give benzaldehyde and toluene (Table 2, entry 4), though with a lower turnover number. The high melting point of 1,3-diphenylacetone (34 °C)[36] restricted the reaction temperature at 60 °C; the higher reaction temperature probably reduces the effective concentration of $(Ph_3P)Rh(ttp)OH$[32] and accounts for the lower efficiency. When the unsymmetric isobutyrophenone was used, the more hindered but weaker (C═O)−^{i}Pr bond (~81.3 kcal mol^{-1})[35] was selectively cleaved over the (C═O)−Ph bond (~97.2 kcal mol^{-1});[35] however, benzaldehyde was catalytically formed instead of benzene (Table 2, entry 5). This is ascribed to the much slower decarbonylation rate in benzoyl radical (PhCO), which has a much lower rate constant of 1.5×10^{-7} s^{-1} at 296 K in comparison to other acyl radicals on the order of 10^4 s^{-1}.[37]

Attempts to develop photocatalytic CCA on aldol-condensable cyclohexanone were unsuccessful. Three reasons have been proposed to account for this observation. First, aldol condensation can be a competitive process to form the conjugated enone, and this consumes the starting material, as Rh(por) can serve as a Lewis acid to catalyze the reaction.[15] Second, the reverse intramolecular ring closing proceeds at a much faster rate than any subsequent intermolecular reactions (Scheme 2). Third, the (C═O)−CH_2R bond is 3 kcal mol^{-1} stronger than the (C═O)−^{i}Pr bond,[35] which makes the CCA more difficult. We have also previously reported that the stoichiometric CCAs of unsubstituted ketones are much less reactive than those of isopropyl ketones.[15] A high temperature of 200 °C is required to achieve CCA in diethyl ketone by Rh(ttp)Me to give Rh(ttp)COEt in 45% yield in 16 days, while the CCA of diisopropyl ketone occurred at 50 °C in 1 day to give Rh(ttp)CO^{i}Pr in 94% yield.[15]

Scheme 2. Fast Intramolecular Ring Closing

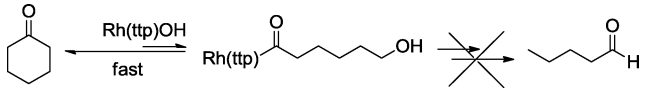

The catalysis was also operative in benzene or acetone solvent, though with slightly lower TOFs (Table 1, entries 10 and 11). This in turn allowed us to follow the reaction progress using ^{1}H NMR spectroscopy. Under the same reaction conditions, H_2 was observed in C_6D_6 by ^{1}H NMR with 17 turnovers in a 1:1 ratio with 2-heptanone (eq 4). This supports the dehydrogenation to give hydrogen.

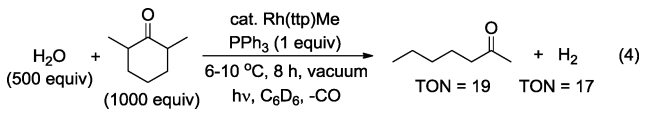

Scheme 3 shows the proposed reaction mechanism using 2,6-dimethylcyclohexanone as the substrate. Photolysis of Rh^{III}(ttp)Me cleaves the Rh−C bond homolytically to give Rh^{II}(ttp).[38] PPh_3 then coordinates to Rh^{II}(ttp) monomer to generate the more electron-rich $(Ph_3P)Rh^{II}$(ttp),[39] which then disproportionates with H_2O to give $(Ph_3P)Rh^{III}$(ttp)OH and Rh^{III}(ttp)H (eq 3).[33] Selective carbon(CO)−C(α) bond activation of 2,6-dimethylcyclohexanone by $(Ph_3P)Rh^{III}$(ttp)-OH occurs through σ-bond metathesis with subsequent dehydrogenation of the alcohol to afford the stoichiometric CCA product Rh^{III}(ttp)$COCH(CH_3)(CH_2)_3COCH_3$.[15] Photolysis further cleaves the Rh−C(CO) bond homolytically to generate the acyl radical **1** and Rh^{II}(ttp) monomer to complete the catalytic cycle. Facile decarbonylation of the acyl radical occurs simultaneously to give the alkyl radical **2**.[37] **2** then undergoes hydrogen atom transfer (HAT) from the bulk 2,6-dimethylcyclohexanone solvent to form 2-heptanone. The decarbonylation accounts for the one-carbon-less 2-heptanone obtained in the photolysis of 2,6-dimethylcyclohexanone. The only exception is in the case of isobutyrophenone; the slow decarbonylation cannot compete with HAT, so that the CO group remains intact (Scheme 4). Finally, the tertiary alkyl radical **3** formed after HAT then abstracts H from Rh(ttp)H to complete the photocatalysis. Overall, there is an anaerobic photocatalytic oxidation of ketone using H_2O with the CCA step involving PPh_3-coordinated rhodium(III) porphyrin hydroxide.[40]

The radical mechanism is supported by a control experiment using (2,2,6,6-tetramethylpiperidin-1-yl)oxyl (TEMPO) as the radical trap. TEMPO significantly retarded the photocatalytic C(CO)−C(α) bond oxidation of 2,6-dimethylcyclohexanone with only 3.5 turnovers obtained under the optimized catalytic conditions (eq 5).

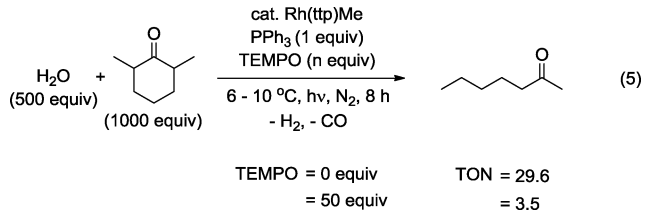

After the photocatalysis, the highly air-sensitive Rh^{II}(ttp) cannot be regenerated. The instability of Rh^{II}(ttp) is attributed to its reaction with O_2 presumably generated from the reduction of Rh^{III}(ttp)OH to give H_2O_2, which further dissociates into H_2O and O_2.[32] The catalyst deactivation also accounts for the limited turnover number observed.

The key steps in the proposed mechanism were supported by independent experiments. The disproportionation of Rh(II) with H_2O was confirmed by $H_2{}^{18}O$ labeling. The photolysis of 2,6-dimethylcyclohexanone with $H_2{}^{18}O$ catalyzed by Rh^{II}(ttp)-Me afforded ^{18}O-enriched 2-heptanone and ^{16}O 2-heptanone in a 4:1 ratio and 27 turnovers (eq 6, Figure S1 in the Supporting

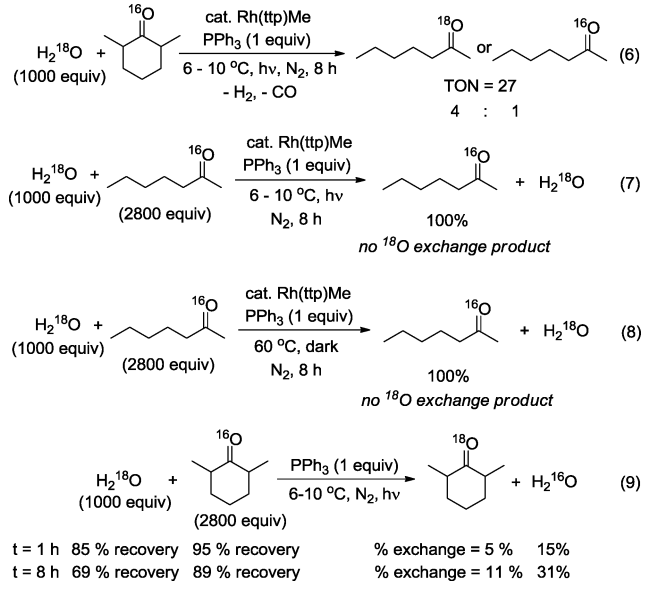

dx.doi.org/10.1021/om400672t | Organometallics 2013, 32, 5391−5401

Scheme 3. Proposed Catalytic Cycle

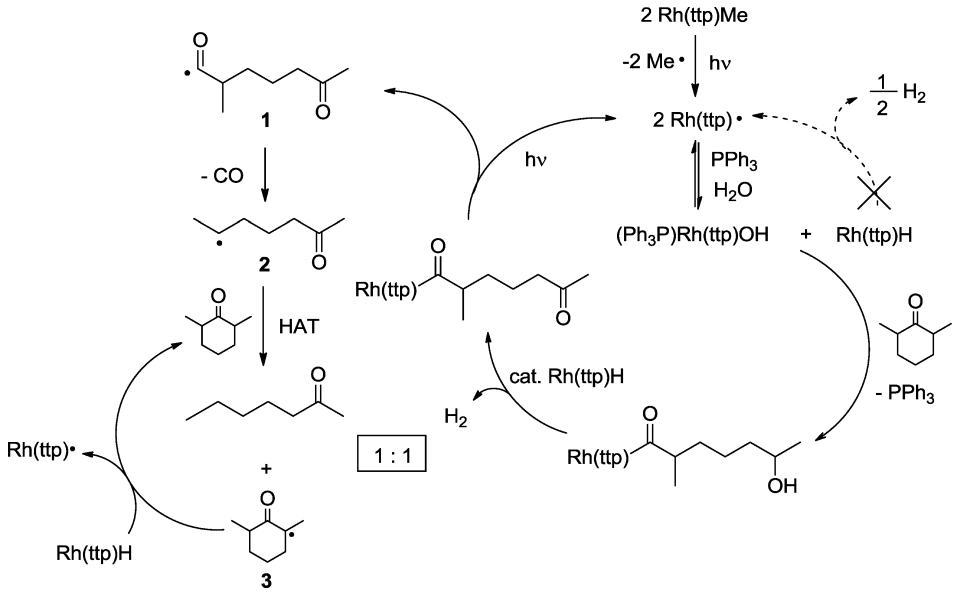

Scheme 4. Slow Decarbonylation in PhCO Radical

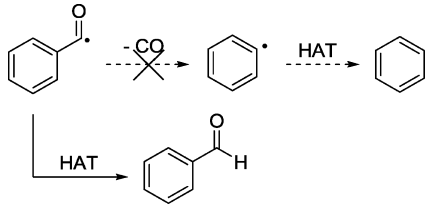

Scheme 5. Acid-Catalyzed $^{16}O/^{18}O$ Exchange and $(Ph_3P)Rh^{III}(ttp)OH$-Catalyzed D_2O and $^{16}O/^{18}O$ Exchange

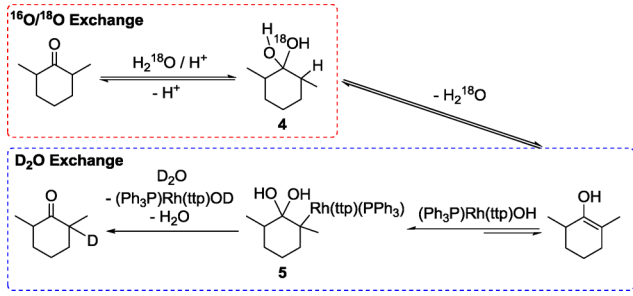

Information). Control experiments were carried out to rule out direct $^{16}O/^{18}O$ exchange on 2-heptanone under both photolytic and thermal conditions, as no ^{18}O enriched 2-heptanone was observed (eqs 7 and 8). This suggests that H_2O is the source of oxygen incorporated in the product.

The partial ^{18}O incorporation in ketone product is attributed to two reasons. First, the commercially available $H_2{}^{18}O$ used is only of 95 atom % ^{18}O enrichment; the presence of $H_2{}^{16}O$ limited the complete incorporation. Second, under the same reaction conditions, the rapid $^{16}O/^{18}O$ exchange of ketone with $H_2{}^{18}O$ was significant. In the control experiment between $H_2{}^{18}O$ and 2,6-dimethylcyclohexanone without Rh(ttp)Me catalyst, the $^{16}O/^{18}O$ exchange occurred in 1 h to give 15% $H_2{}^{16}O$ (eq 9). At the end of 8 h, the recovery yield of $H_2{}^{18}O$ was 69% and $H_2{}^{16}O$ contributes to the remaining 31% water content in the reaction mixture (eq 9). In the photocatalytic CCA of 2,6-dimethylcyclohexanone catalyzed by Rh(ttp)Me, a small amount of $H_2{}^{16}O$ formed from exchange acts as the oxidant during the course of the reaction and this accounts for the ^{16}O-2-heptanone (20%) observed after photolysis. It should be noted that the ^{18}O exchanged into the carbonyl oxygen of 2,6-dimethylhexanone yields $C^{18}O$ and does not affect the ^{18}O content of 2-heptanone.

A mechanism via a geminal diol intermediate can account for the increased reactivity of 2,6-dimethylcyclohexanone in the $^{16}O/^{18}O$ exchange in comparison to that of 2-heptanone (Scheme 5). In six-membered cyclic ketones, the trigonal-planar carbonyl carbon distorts the stable chair conformation of six-membered rings, making it more favorable to exchange into a germinal diol.[41] Acid and $(Ph_3P)Rh(ttp)OH$ (also a Lewis acid) catalyze the addition of $H_2{}^{18}O$ to form the geminal diol hydrates **4** and **5** and transform the trigonal carbon to a tetrahedral configuration. The extra stability gained from restoring the distortion of the chair conformation in the transition state leads to a more favorable addition reaction.

The photocatalytic dehydrogenation of alcohol under alkaline conditions with rhodium porphyrin complex has been reported by Saito et al. to yield a ketone and H_2.[20] The successful detection of H_2 in the photocatalyic carbon−carbon bond oxidation of 2,6-dimethylcyclohexanone (eq 4, Figure S2 in the Supporting Information) supports the step of alcohol dehydrogenation into ketone.[42] The generation of a stoichiometric amount of H_2 from the photolysis of $Rh^{III}(ttp)H$ (eq 10) is not likely, since it proceeded much more slowly than the

$$2Rh(ttp)H \xrightarrow[\text{Benzene}]{\text{4 h, h}\nu} Rh_2(ttp)_2 + H_2 \qquad (10)$$

photocatalytic carbon−carbon bond oxidation of ketones. The former required at least 4 h for completeness in benzene,[43] while the latter occurred in 30 turnovers within 8 h. Furthermore, 1.5 equiv of H_2 would be observed if homolytic cleavage of (ttp)Rh−H for H_2 generation was operating according to the reaction stoichiometry (Scheme 3, dotted arrow). In this system, H_2 and 2-heptanone were observed in a nearly 1:1 ratio (eq 4). Therefore, this pathway can be ruled out.

dx.doi.org/10.1021/om400672t | Organometallics 2013, 32, 5391−5401

We favor Rh(ttp)H as the complex for the catalytic dehydrogenation of alcohol on the basis of the following three reasons. (1) Rhodium porphyrin hydride is a known photocatalyst for the dehydrogenation of alcohol into ketone under alkaline conditions.[20] (2) Rh^{II}(ttp) is highly reactive toward water in the presence of Ph_3P and is therefore very low in equilibrium concentration in the disproportionation reaction. The alcohol intermediate is also much lower in concentration than ketone substrates and water. Therefore, the catalytic role of Rh^{II}(ttp) in the dehydrogenation process is disfavored on the basis of concentration considerations. (3) (Ph_3P)Rh(ttp)OH, though very reactive, can react with an alcohol (2-propanol) to give either (Ph_3P)Rh(ttp)$OCH(Me)_2$ or (Ph_3P)Rh(ttp)C-$(OH)(Me)_2$. However, the β-hydride elimination of these two species to give acetone and (Ph_3P)Rh(ttp)H is reasoned to be slow, as the rate of 1,2-rearrangement of Rh(bocp)-CH_2CH_2Ph (bocp = 2,3,7,8,12,13,17,18-octachloro-5,10,15,20-tetrakis(p-tert-butylphenyl)porphyrinato dianion) into Rh(bocp)CH(Me)Ph via β-H elimination is slowed down by PPh_3 coordination.[44] Furthermore, (Ph_3P)Rh(ttp)H or Rh(ttp)H is regenerated from β-H elimination and can catalyze the dehydrogenation reaction on the basis of (1). Therefore, Rh(ttp)H is the favored dehydrogenation catalyst on the basis of concentration and mechanistic simplicity considerations.

A D_2O labeling experiment revealed that the HAT by the secondary alkyl radical **2** formed from the decarbonylation is from the bulk ketone rather than from Rh(ttp)H, due to the much higher concentration of ketone (Scheme 3). The α-carbonyl-substituted tertiary alkyl radical **3** forms then abstracts the deuterium atom from Rh^{III}(ttp)D and Rh^{II}(ttp) is then recycled (Scheme 3, eq 11). The ΔH value of this HAT is the

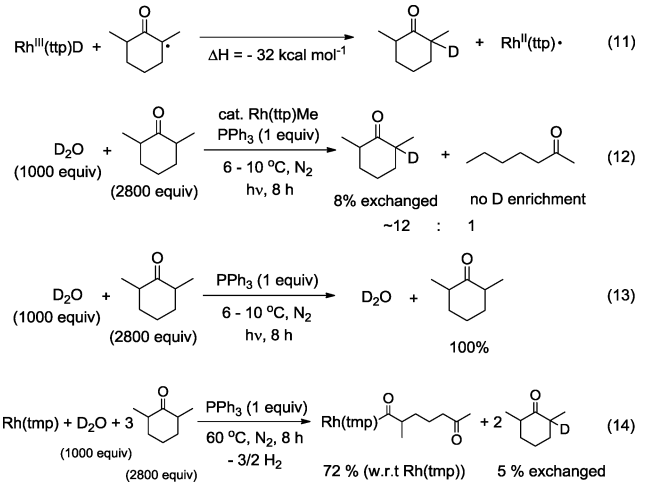

difference between the bond dissociation enthalpy of the α-C–H bond of 2,6-dimethylcyclohexanone (92 kcal mol^{-1})[35] and that of Rh(ttp)–H (60 kcal mol^{-1}).[35] The occurrence of this exothermic HAT process (ΔH = −32 kcal mol^{-1}) was supported by the d_1-enriched 2,6-dimethylcyclohexanone observed in 8% yield after the photocatalysis by Rh(ttp)Me (eq 12). Control experiments without Rh(ttp)Me catalyst also showed that no direct photoinduced exchange of D_2O with 2,6-dimethylcyclohexanone occurred (eq 13). In neutral medium without rhodium porphyrin species, the proton concentration is not high enough to catalyze the D_2O exchange.

Since d_1-enriched 2,6-dimethylcyclohexanone and 2-heptanone were observed in a 12:1 ratio in the photocatalytic carbon–carbon bond oxidation (eq 12), we propose the (Ph_3P)Rh(ttp)OH-catalyzed D_2O exchange of 2,6-dimethylcyclohexanone predominates (Scheme 5). Photochemical acid-catalyzed D_2O exchange has been reported to proceed via an enol intermediate.[45] The enol form of 2,6-dimethylcyclohexanone first undergoes syn addition reaction with (Ph_3P)Rh(ttp)OH to give the bis-addition product **5**, and it is further hydrolyzed by D_2O rapidly to yield the α-D-2,6-dimethylcyclohexanone. The addition of water-soluble rhodium porphyrin hydroxide to an electron-rich alkene has been reported by Wayland and Fu;[46] the regioselectivity of our proposed intermediate **5** is consistent with their observations. Indeed, under thermal conditions, the stoichiometric CCA of 2,6-dimethylcyclohexanone occurred together with (Ph_3P)-Rh^{II}(tmp)OH-catalyzed D_2O exchange. Analyzing the crude reaction mixture revealed that 5% of d_1-enriched 2,6-dimethylcyclohexanone was generated (eq 14). Therefore, the D_2O exchange pathway via $(Ph_3P)Rh^{II}$(ttp)OH addition accounts for the excess d_1-enriched 2,6-dimethylcyclohexanone obtained in the catalysis.

To gain a further mechanistic understanding of the CCA step, we have conducted kinetic studies on the stoichiometric reaction of diisopropyl ketone with the synthetically more accessible and well-studied Rh^{II}(tmp) monomer,[14] which gave a high yield of 90% of Rh^{III}(tmp)CO^iPr within 10 min in benzene cleanly (eq 15). There was no side reaction to

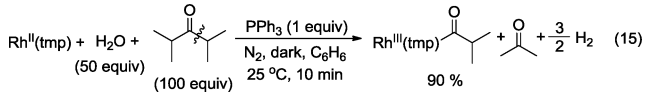

interfere with subsequent mechanistic studies. Kinetic measurements were then undertaken by UV/vis spectroscopy, with initial concentrations of diisopropyl ketone kept in at least 10-fold excess with reference to Rh^{II}(tmp) to establish the pseudo-first-order conditions. The absorbances at 549 nm were monitored and analyzed to follow a first-order exponential increase (Figure 1). The kinetic data were then fitted by first-order exponential growth using OriginPro 7.5 software. A typical pseudo-first-order curve is shown in Figure 1.

Saturation kinetics was observed on [PPh_3], suggesting the rapid pre-equilibrium of triphenylphosphine coordination to rhodium center prior to the rate-determining step (Figure 2). First-order kinetics were observed for both [Rh^{II}(tmp)] and [$^iPr_2C{=}O$] (Figures 1 and 3). The first-order rate constant k

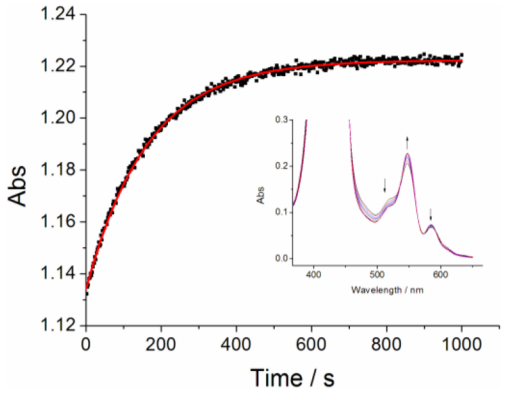

Figure 1. Typical timescan taken at the wavelength where maximum absorbance change occurs (549 nm). Inset: spectral changes from 300 to 800 nm.

dx.doi.org/10.1021/om400672t | Organometallics 2013, 32, 5391–5401

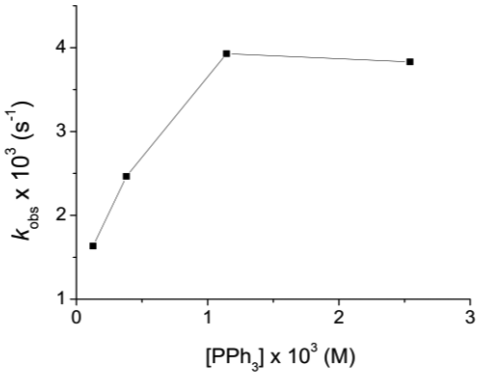

Figure 2. Saturation kinetics on [PPh_3].

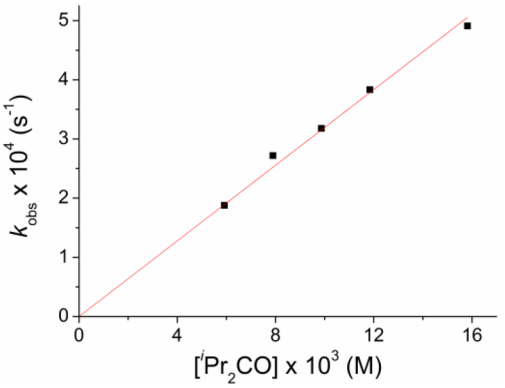

Figure 3. Linear relationship between k_{obs} and [^{i}Pr$_2$C═O].

(25 °C) was evaluated to be (3.2 ± 0.2) × 10^{-2} M^{-1} s^{-1} (Table 3, Figure 3). No dependence on [H_2O] was observed by

Table 3. Observed Rate Constants at Different [^{i}Pr$_2$C═O]

entry[a]	[^{i}Pr$_2$C═O] (10^4 M)	k_{obs} (10^3 s^{-1})	error (10^5 s^{-1})
1	5.92	1.87	0.95
2	7.89	2.71	1.02
3	9.87	3.18	3.42
4	11.8	3.83	4.35
5	15.8	4.91	6.16

[a]Reaction conditions: [Rh(tmp)] = 1.49 × 10^{-5} M, [^{i}Pr$_2$C═O] = (3.95–15.8) × 10^{-4} M, [PPh_3] = 1.91 × 10^{-3} M, [H_2O] = 3.74 × 10^{-2} M, temperature 25 °C.

quadrupling the concentration of water, suggesting that the disproportionation reaction rate is fast. The overall second-order kinetics suggest a bimolecular reaction between a Ph_3P-coordinated Rh(tmp) derivative and ^{i}Pr$_2$C═O in the rate-determining step. The overall rate law is shown in eq 16, where k_{obs} = k[^{i}Pr$_2$C═O].

$$\text{rate} = k[\text{Rh}^{\text{II}}(\text{tmp})][^i\text{Pr}_2\text{C}{=}\text{O}] = k_{obs}[\text{Rh}^{\text{II}}(\text{tmp})] \quad (16)$$

Further analysis of the activation parameters obtained from the rate constants yielded $\Delta S^{\ddagger}_{obs}$ = −5.42 ± 0.35 cal K^{-1} mol^{-1}, $\Delta H^{\ddagger}_{obs}$ = 14.88 ± 0.82 kcal mol^{-1}, and $\Delta G^{\ddagger}_{obs}$ = 16.50 ± 1.07 kcal mol^{-1} (Figure 4 and Table 4). The negative $\Delta S^{\ddagger}_{obs}$ value suggests an associative transition state in the rate-determining CCA step.

A kinetic scheme consistent with the rate law is proposed (eq 17, where [Rh(tmp)]$_0$ is the initial concentration of Rh(tmp),

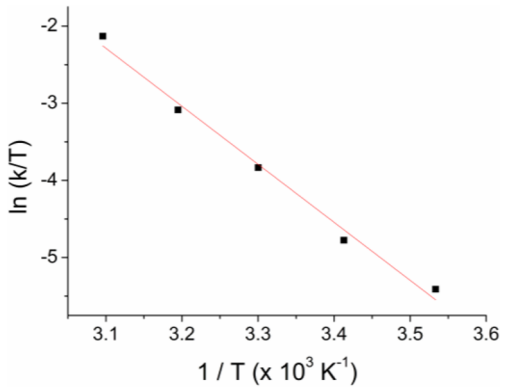

Figure 4. Eyring plot of the reaction between Rh(tmp) and ^{i}Pr$_2$C═O in benzene from 10 to 50 °C.

Table 4. Observed Relationship between k_{obs} and Temperature

entry[a]	T (°C)	T (K)	$1/T$ (10^3 K^{-1})	k_{obs} (10^3 s^{-1})	error of k_{obs} (10^5 s^{-1})	k (M^{-1} s^{-1})	ln (k/T)
1	10	283	3.53	2.07	1.97	1.31	−5.41
2	20	293	3.41	4.03	2.31	2.55	−4.78
3	30	303	3.30	10.3	2.32	6.55	−3.83
4	40	313	3.19	22.6	4.14	14.3	−3.09
5	50	323	3.10	60.5	19.3	38.3	−2.13

[a]Reaction conditions: [Rh(tmp)] = 2.97 × 10^{-5} M, [^{i}Pr$_2$C═O] = 2.23 × 10^{-3} M, [PPh_3] = 1.91 × 10^{-3} M, [H_2O] = 3.74 × 10^{-2} M, temperature 10–50 °C

$$\text{rate} = \frac{k_3K_1[\text{PPh}_3]}{(1 + K_1[\text{PPh}_3])}[\text{Rh(tmp)}]_0[^i\text{Pr}_2\text{C}{=}\text{O}] \quad (17)$$

and Scheme 6).[47] PPh_3 first coordinates to Rh^{II}(tmp) to give the more electron rich (Ph_3P)Rh^{III}(tmp), and it undergoes disproportionation with H_2O very rapidly to generate (Ph_3P)-Rh^{III}(tmp)OH and Rh^{III}(tmp)H. The six-coordinate (Ph_3P)-Rh^{III}(tmp)OH then cleaves the carbon–carbon bond of diisopropyl ketone, with the diisopropyl ketone and OH group on the same face of the porphyrin plane in the transition state TS1, to give Rh(tmp)CO^{i}Pr and 2-propanol. CHA of 2-propanol by Rh(tmp)H generates the rhodium porphyrin alkyl **6** and hydrogen. Subsequently, **6** undergoes β-H elimination to give acetone to complete the stoichiometry and Rh(tmp)H is regenerated. Finally, Rh^{III}(tmp)H is recycled by reacting with diisopropyl ketone at the α-C–H bond and subsequent rapid hydrolysis produces (Ph_3P)Rh^{III}(tmp)OH in the presence of PPh_3.[48] Therefore, Rh(tmp)H catalyzes the dehydrogenation of 2-propanol to acetone.

We also consider other possible transition states in the key carbon–carbon bond activation step. Since keto–enol tautomerization is significant in ketone substrates, (Ph_3P)Rh-(tmp)OH can add to the enol isomer of diisopropyl ketone via TS2 (Scheme 7). The β-H elimination generates Rh(tmp)H and the hydroxylated ketone. Rh(tmp)H then cleaves the C(CO)–C(α) bond of the ketone through σ-bond metathesis to yield Rh–acyl and 2-propanol. Indeed, the addition of [Rh^{II}(oep)]$_2$ (oep = octaethylporphyrinato dianion) to the enol isomer of an aldehyde or ketone to generate an alkyl -bridged complex and the subsequent β-O–H migration has been reported by Wayland et al.[49] However, we favor TS1 to be the

dx.doi.org/10.1021/om400672t | Organometallics 2013, 32, 5391–5401

Scheme 6. Proposed Mechanistic Scheme for Stoichiometric CCA

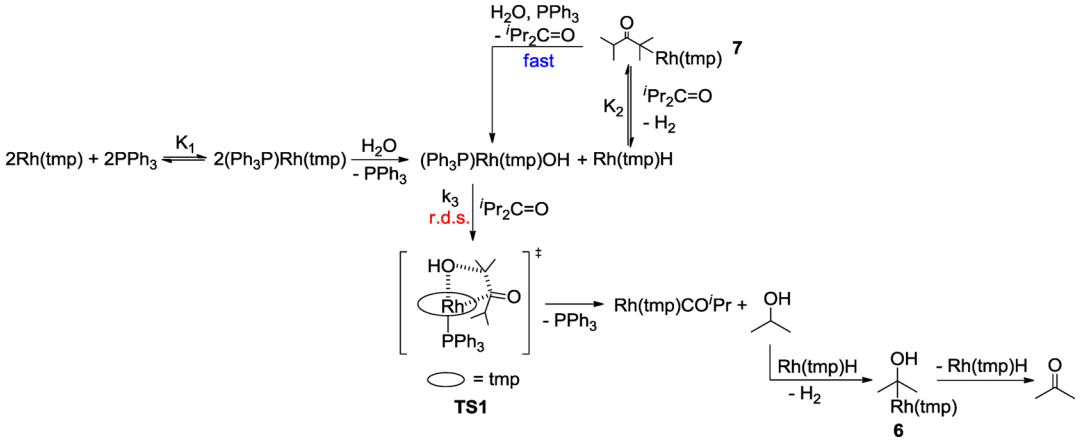

Scheme 7. Addition of $(Ph_3P)Rh(tmp)OH$ to Enol Isomer of Diisopropyl Ketone

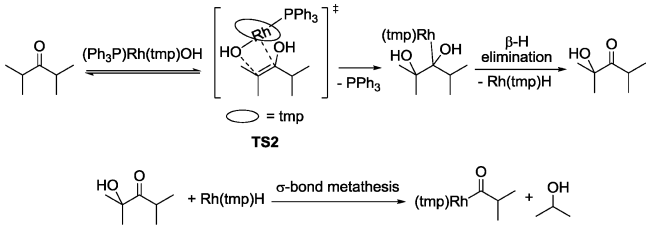

more probable transition state due to mechanistic simplicity and generality, as the CCA of ethers which bear no enolizable form is also successful.[7]

Concerning the CCA step, this type of cis six- or seven-coordinate transition state (TS1) of a metalloporphyrin bearing two cis reacting ligands, while uncommon, is not unprecedented. The X-ray structure of the six-coordinated cis oxo peroxo tungsten porphyrin complex has been reported.[50] The sterically crowded transition states are possible and have been mentioned in the C−H insertion reaction of 1,4-cyclohexadiene using the six-coordinated MeIr(ttp)=CR_1R_2 complexes with Ir−C bond lengthening.[51] A seven-coordinated transition state was suggested, though not favored, in the cyclopropanation with olefin[52] using MeIr(ttp)=CHR catalyst. The presence of a cis coordination site in metalloporphyrins is known in various systems;[53] the *cis*-disubstituted metalloporphyrin transition state (TS1) allows the reaction to proceed in a concerted σ-bond metathesis manner. Indeed, the steric congestion in the transition state can presumably be reduced by the longer (tmp)Rh−OH bond length in $(Ph_3P)Rh(tmp)OH$. The bond length of (tmp)Rh−OH is estimated to be 2.2 Å,[54] in comparison to 2.1 Å for a typical (tmp)Rh−R bond. This slightly longer bond length in $(Ph_3P)Rh(tmp)OH$, bearing a small OH ligand, allows the easier approach of ketone molecules and subsequently the σ-bond metathesis occurs.

In photocatalysis, the (ttp)Rh−C(O)R cleavage is likely faster than the reaction of Rh(ttp)H with 2,6-dimethylcyclohexanone, which occurs by a crowded four-centered transition state through σ-bond metathesis. Therefore, the resultant acyl or alkyl radical undergoes HAT with ketone substrate to give an α-carbonyl carbon centered radical to consume Rh(ttp)H via a secondary HAT reaction. Thus, the ratio of organic ketones and H_2 is 1:1 (Scheme 3). In the stoichiometric reaction, Rh(tmp)CO^{i}Pr is stable. Rh(tmp)H is thus consumed by the direct CHA reaction with diisopropyl ketone at the α-carbonyl−hydrogen bond to generate the rhodium porphyrin secondary alkyl species **7** and hydrogen. Further hydrolysis of **7** regenerates $(Ph_3P)Rh(tmp)OH$ and diisopropyl ketone. Since hydrogen is generated from both the dehydrogenation of 2-propanol and the direct CHA of diisopropyl ketone by Rh(tmp)H according to the stoichiometry, the ratio of Rh(tmp)CO^{i}Pr to H_2 is therefore 2:3 from a stoichiometry analysis, though the concentration of H_2 is too low to allow an accurate determination.

CONCLUSIONS

In conclusion, photocatalytic carbon−carbon bond anaerobic oxidation of isopropyl and benzyl ketones was achieved under ambient conditions. $(Ph_3P)Rh(ttp)OH$ is the proposed intermediate to cleave the carbon−carbon bond in the rate-determining step. H_2O serves as an oxygen source to oxidize the $C(sp^3)$−C(CO) bond of ketones. Further studies are ongoing.

EXPERIMENTAL SECTION

General Procedures. All materials were obtained from commercial suppliers and used without further purification unless otherwise specified. Benzene was distilled from sodium under nitrogen. Porphyrins and metalloporphyrins were prepared according to the literature procedures, and they have been characterized.[55−58] All solutions used were degassed three times by freeze−thaw−pump cycles and stored in a Teflon screwhead stoppered flask, which was wrapped with aluminum foil to protect from light.

Thin-layer chromatography was performed on Merck precoated silica gel 60 F_{254} plates. Silica gel (Merck, 70−230 mesh) was used for column chromatography.

Physical and Analytical Measurements. ^{1}H NMR spectra were recorded on a Bruker AvanceIII 400 instrument at 400 MHz or a Bruker AvanceIII 700 instrument at 700 MHz. Chemical shifts were referenced internally to the residual proton resonance in C_6D_6 (δ 7.15 ppm) or $CDCl_3$ (δ 7.26 ppm) or with tetramethylsilane ($(TMS)_4Si$, δ 0.00 ppm) as the internal standard. ^{13}C NMR spectra were recorded on a Bruker AvanceIII 700 instrument at 175 MHz. Chemical shifts were referenced internally to the residual proton resonance in $CDCl_3$ (δ 77.16 ppm) as the internal standard. Chemical shifts (δ) are reported as parts per million (ppm) in the δ scale downfield from TMS. Coupling constants (J) are reported in hertz (Hz).

GC-MS analyses were conducted on a GCMS-QP2010 Plus system using an Rtx-5MS column (30 m × 0.25 mm). Details of the GC program are as follows. The column oven temperature and injection temperature were 50.0 and 250 °C. Helium was used as the carrier gas. The flow control mode was chosen as linear velocity (36.3 cm s^{-1})

dx.doi.org/10.1021/om400672t | *Organometallics* 2013, 32, 5391−5401

with a pressure of 53.5 kPa. The total flow, column flow, and purge flow were 24.0, 1.0, and 3.0 mL min^{-1}, respectively. Split mode injection with a split ratio of 20.0 was applied. After injection, the column oven temperature was kept at 50 °C for 5 min and was then elevated at a rate of 30 °C min^{-1} for 10 min until 250 °C. The temperature of 250 °C was kept for 5 min. The retention time and mass spectrum of organic products obtained were identical with those of commercially available authentic samples.

The photolysis was carried out using a 400 W Philips halide lamp with a water circulation system to control the reaction temperature. The light source and the reaction flask were kept at a distance of 5 cm from each other.

The UV analysis was performed on a Hitachi U-3300 UV−vis spectrophotometer equipped with a Neslab RTE-110 temperature controller. Water was used as the circulating liquid. The scans were carried out at temperatures ranging from 10.0 (±0.2) °C to 50.0 (±0.2) °C. The temperatures were measured by a thermocouple wire placed in an adjacent blank UV cell which was filled with benzene and placed inside the sample compartment. The UV spectra were scanned at 600 nm/min between 350 and 800 nm, and the experimental absorbance was measured at 530 nm. UV data were analyzed with the software OriginPro 7.5 from OriginLab Corp.

Experimental Procedures. *Photolysis of 2,6-Dimethylcyclohexanone with Rh(tmp)Me and H_2O (500 equiv) at 25−30 °C for 8 h.* Rh(tmp)Me (1.0 mg, 0.0011 mmol) and H_2O (10 μL, 0.556 mmol) were dissolved in 2,6-dimethylcyclohexanone (500 μL). The reaction mixture was degassed three times by freeze−thaw−pump cycles, purged with N_2, and photolyzed at 25−30 °C under nitrogen for 8 h. The crude solution was collected by vacuum distillation and analyzed by GC/MS. 2-Heptanone was obtained in 9 turnovers using naphthalene as the internal standard. 2-Heptanone: t_R = 7.186 min. EIMS: *m*/*z* (relative %) 114 (1), 99 (1), 85 (1), 71 (2), 59 (1), 58 (7), 43 (10), 41 (1).

Photolysis of 2,6-Dimethylcyclohexanone with Rh(tmp)Me, H_2O (500 equiv), and PPh_3 (1 equiv) at 25−30 °C for 8 h. Rh(tmp)Me (1.0 mg, 0.0011 mmol), H_2O (10 μL, 0.556 mmol), and PPh_3 (0.3 mg, 0.0011 mmol) were dissolved in 2,6-dimethylcyclohexanone (500 μL). The reaction mixture was degassed three times by freeze−thaw−pump cycles, purged with N_2, and photolyzed at 25−30 °C under nitrogen for 8 h. The crude solution was collected by vacuum distillation and analyzed by GC/MS. 2-Heptanone was obtained in 12.6 turnovers using naphthalene as the internal standard.

Photolysis of 2,6-Dimethylcyclohexanone with Rh(ttp)Me, H_2O (500 equiv), and PPh_3 (1 equiv) at 25−30 °C for 8 h. Rh(ttp)Me (1.0 mg, 0.0013 mmol), H_2O (11 μL, 0.611 mmol), and PPh_3 (0.3 mg, 0.0011 mmol) were dissolved in 2,6-dimethylcyclohexanone (500 μL). The reaction mixture was degassed three times by freeze−thaw−pump cycles, purged with N_2, and photolyzed at 25−30 °C under nitrogen for 8 h. The crude solution was collected by vacuum distillation and analyzed by GC/MS. 2-Heptanone was obtained in 21.1 turnovers using naphthalene as the internal standard.

Photolysis of 2,6-Dimethylcyclohexanone with Rh(ttp)Me and H_2O (500 equiv) at 25−30 °C for 8 h. Rh(ttp)Me (1.0 mg, 0.0013 mmol) and H_2O (11 μL, 0.611 mmol) was dissolved in 2,6-dimethylcyclohexanone (500 μL). The reaction mixture was degassed three times by freeze−thaw−pump cycles, purged with N_2, and photolyzed at 25−30 °C under nitrogen for 8 h. The crude solution was collected by vacuum distillation and analyzed by GC/MS. 2-Heptanone was obtained in 11.3 turnovers using naphthalene as the internal standard.

Photolysis of 2,6-Dimethylcyclohexanone with Rh(ttp)Me, H_2O (500 equiv), and PPh_3 (1 equiv) at 50−60 °C for 8 h. Rh(ttp)Me (1.0 mg, 0.0013 mmol), H_2O (11 μL, 0.611 mmol), and PPh_3 (0.3 mg, 0.0011 mmol) were dissolved in 2,6-dimethylcyclohexanone (500 μL). The reaction mixture was degassed three times by freeze−thaw−pump cycles, purged with N_2, and photolyzed at 50−60 °C under nitrogen for 8 h. The crude solution was collected by vacuum distillation and analyzed by GC/MS. 2-Heptanone was obtained in 15.9 turnovers using naphthalene as the internal standard.

Photolysis of 2,6-Dimethylcyclohexanone with Rh(ttp)Me, H_2O (500 equiv), and PPh_3 (1 equiv) at 6−10 °C for 8 h. Rh(ttp)Me (1.0 mg, 0.0013 mmol), H_2O (11 μL, 0.611 mmol), and PPh_3 (0.3 mg, 0.0011 mmol) were dissolved in 2,6-dimethylcyclohexanone (500 μL). The reaction mixture was degassed three times by freeze−thaw−pump cycles, purged with N_2, and photolyzed at 6−10 °C under nitrogen for 8 h. The crude solution was collected by vacuum distillation and analyzed by GC/MS. 2-Heptanone was obtained in 29.6 turnovers using naphthalene as the internal standard.

Photolysis of 2,6-Dimethylcyclohexanone with Rh(ttp)Me, H_2O (50 equiv), and PPh_3 (1 equiv) at 6−10 °C for 8 h. Rh(ttp)Me (1.0 mg, 0.0013 mmol), H_2O (1 μL, 0.056 mmol), and PPh_3 (0.3 mg, 0.0011 mmol) were dissolved in 2,6-dimethylcyclohexanone (500 μL). The reaction mixture was degassed three times by freeze−thaw−pump cycles, purged with N_2, and photolyzed at 6−10 °C under nitrogen for 8 h. The crude solution was collected by vacuum distillation and analyzed by GC/MS. 2-Heptanone was obtained in 7.8 turnovers using naphthalene as the internal standard.

Photolysis of 2,6-Dimethylcyclohexanone with Rh(ttp)Me, H_2O (100 equiv), and PPh_3 (1 equiv) at 6−10 °C for 8 h. Rh(ttp)Me (1.0 mg, 0.0013 mmol), H_2O (2 μL, 0.111 mmol), and PPh_3 (0.3 mg, 0.0011 mmol) were dissolved in 2,6-dimethylcyclohexanone (500 μL). The reaction mixture was degassed three times by freeze−thaw−pump cycles, purged with N_2, and photolyzed at 6−10 °C under nitrogen for 8 h. The crude solution was collected by vacuum distillation and analyzed by GC/MS. 2-Heptanone was obtained in 9.5 turnovers using naphthalene as the internal standard.

Photolysis of 2,6-Dimethylcyclohexanone with Rh(ttp)Me, H_2O (1000 equiv), and PPh_3 (1 equiv) at 6−10 °C for 8 h. Rh(ttp)Me (1.0 mg, 0.0013 mmol), H_2O (22 μL, 1.222 mmol), and PPh_3 (0.3 mg, 0.0011 mmol) were dissolved in 2,6-dimethylcyclohexanone (500 μL). The reaction mixture was degassed three times by freeze−thaw−pump cycles, purged with N_2, and photolyzed at 6−10 °C under nitrogen for 8 h. The crude solution was collected by vacuum distillation and analyzed by GC/MS. 2-Heptanone was obtained in 31.0 turnovers using naphthalene as the internal standard.

Photolysis of 2,6-Dimethylcyclohexanone with H_2O (500 equiv) and PPh_3 (1 equiv) at 50−60 °C for 8 h. H_2O (11 μL, 0.611 mmol) and PPh_3 (0.3 mg, 0.0011 mmol) were dissolved in 2,6-dimethylcyclohexanone (500 μL). The reaction mixture was degassed three times by freeze−thaw−pump cycles, purged with N_2, and photolyzed at 50−60 °C under nitrogen for 8 h. The crude solution was collected by vacuum distillation and analyzed by GC/MS. No 2-heptanone was obtained.

Photolysis of 2,6-Dimethylcyclohexanone with Rh(ttp)Me, H_2O (500 equiv), and PPh_3 (1 equiv) in Benzene at 6−10 °C for 8 h. Rh(ttp)Me (1.0 mg, 0.0013 mmol), 2,6-dimethylcyclohexanone (175 μL, 1.25 mmol), H_2O (11 μL, 0.611 mmol), and PPh_3 (0.3 mg, 0.0011 mmol) were dissolved in benzene (325 μL). The reaction mixture was degassed three times by freeze−thaw−pump cycles, purged with N_2, and photolyzed at 6−10 °C under nitrogen for 8 h. The crude solution was collected by vacuum distillation and analyzed by GC/MS. 2-Heptanone was obtained in 19.3 turnovers using naphthalene as the internal standard.

Photolysis of 2,6-Dimethylcyclohexanone with Rh(ttp)Me, H_2O (500 equiv), and PPh_3 (1 equiv) in Acetone at 6−10 °C for 8 h. Rh(ttp)Me (1.0 mg, 0.0013 mmol), 2,6-dimethylcyclohexanone (175 μL, 1.25 mmol), H_2O (11 μL, 0.611 mmol), and PPh_3 (0.3 mg, 0.0011 mmol) were dissolved in acetone (325 μL). The reaction mixture was degassed three times by freeze−thaw−pump cycles, purged with N_2, and photolyzed at 6−10 °C under nitrogen for 8 h. The crude solution was collected by vacuum distillation and analyzed by GC/MS. 2-Heptanone was obtained in 18.6 turnovers using naphthalene as the internal standard.

Photolysis of Diisopropyl Ketone with Rh(ttp)Me, H_2O (500 equiv), and PPh_3 (1 equiv) at 6−10 °C for 8 h. Rh(ttp)Me (1.0 mg, 0.0013 mmol), H_2O (22 μL, 1.222 mmol), and PPh_3 (0.3 mg, 0.0011 mmol) were dissolved in diisopropyl ketone (500 μL). The reaction mixture was degassed three times by freeze−thaw−pump cycles, purged with N_2, and photolyzed at 6−10 °C under nitrogen for 8 h. The crude solution was collected by vacuum distillation and analyzed

by GC/MS. Acetone was obtained in 8.9 turnovers using naphthalene as the internal standard. Acetone: t_R = 2.153 min. EIMS: m/z (relative %) 58 (3), 43 (10).

Photolysis of 2-Methylcyclohexanone with Rh(ttp)Me, H_2O (500 equiv), and PPh_3 (1 equiv) at 6−10 °C for 8 h. Rh(ttp)Me (1.0 mg, 0.0013 mmol), H_2O (11 μL, 0.611 mmol), and PPh_3 (0.3 mg, 0.0011 mmol) were dissolved in 2-methylcyclohexanone (500 μL). The reaction mixture was degassed three times by freeze−thaw−pump cycles, purged with N_2, and photolyzed at 6−10 °C under nitrogen for 8 h. The crude solution was collected by vacuum distillation and analyzed by GC/MS. 2-Hexanone was obtained in 13.9 turnovers using naphthalene as the internal standard. 2-Hexanone: t_R = 5.839 min. EIMS: m/z (relative %) 100 (1), 85 (1), 58 (5), 57 (2), 43 (10), 41 (2).

Photolysis of 1,3-Diphenylacetone with Rh(ttp)Me, H_2O (500 equiv), and PPh_3 (1 equiv) at 6−10 °C for 8 h. Rh(ttp)Me (1.0 mg, 0.0013 mmol), H_2O (22 μL, 1.222 mmol), and PPh_3 (0.3 mg, 0.0011 mmol) were dissolved in 1,3-diphenylacetone (500 μL). The reaction mixture was degassed three times by freeze−thaw−pump cycles, purged with N_2, and photolyzed at 50−60 °C under nitrogen for 8 h. The crude solution was collected by vacuum distillation and analyzed by GC/MS. Benzaldehyde and toluene were observed in 4.9 and 1.3 turnovers, respectively, using benzene as the internal standard. Benzaldehyde: t_R = 8.739 min. EIMS: m/z (relative %) 106 (10), 105 (9), 78 (2), 77 (10), 51 (5), 50 (3); Toluene: t_R = 6.239 min. EIMS: m/z (relative %) 92 (6), 91 (10), 65 (1).

Photolysis of Isobutyrophenone with Rh(ttp)Me, H_2O (500 equiv), and PPh_3 (1 equiv) at 6−10 °C for 8 h. Rh(ttp)Me (1.0 mg, 0.0013 mmol), H_2O (22 μL, 1.222 mmol), and PPh_3 (0.3 mg, 0.0011 mmol) were dissolved in isobutyrophenone (500 μL). The reaction mixture was degassed three times by freeze−thaw−pump cycles, purged with N_2, and photolyzed at 6−10 °C under nitrogen for 8 h. The crude solution was collected by vacuum distillation and analyzed by GC/MS. Acetone and benzaldehyde were obtained in 3.9 and 4.9 turnovers, respectively, using benzene as the internal standard. Acetone: t_R = 2.153 min. EIMS: m/z (relative %) 58 (3), 43 (10); Benzaldehyde: t_R = 8.735 min. EIMS: m/z (relative %) 106 (10), 105 (9), 78 (2), 77 (10), 51 (5), 50 (3).

Photolysis of Cyclohexanone with Rh(ttp)Me, H_2O (500 equiv), and PPh_3 (1 equiv) at 6−10 °C for 8 h. Rh(ttp)Me (1.0 mg, 0.0013 mmol), H_2O (22 μL, 1.222 mmol), and PPh_3 (0.3 mg, 0.0011 mmol) were dissolved in cyclohexanone (500 μL). The reaction mixture was degassed three times by freeze−thaw−pump cycles, purged with N_2, and photolyzed at 6−10 °C under nitrogen for 8 h. The crude solution was collected by vacuum distillation and analyzed by GC/MS. No organic product was obtained.

Sealed NMR Tube Experiment for the Photolysis of 2,6-Dimethylcyclohexanone with Rh(ttp)Me, H_2O (500 equiv), and PPh_3 (1 equiv) in Benzene-d_6 at 6−10 °C for 8 h. Rh(ttp)Me (1.0 mg, 0.0013 mmol), 2,6-dimethylcyclohexanone (175 μL, 1.25 mmol), H_2O (11 μL, 0.611 mmol), and PPh_3 (0.3 mg, 0.0011 mmol) were dissolved in benzene-d_6 (325 μL). The reaction mixture was degassed three times by freeze−thaw−pump cycles and the tube flame-sealed under vacuum. After the reaction tube was photolyzed at 6−10 °C for 8 h, it was analyzed by ^{1}H NMR. H_2 was observed in 17 turnovers. ^{1}H NMR (C_6D_6, 400 MHz): δ 4.46, (s, 2 H). The crude mixture was then transferred to another tube to collect 2,6-dimethylcyclohexanone by vacuum distillation. The crude solution was analyzed by GC/MS, and 2-heptanone was obtained in 19 turnovers using naphthalene as the internal standard.

Photolysis of 2,6-Dimethylcyclohexanone with Rh(ttp)Me, $H_2{}^{18}O$ (1000 equiv), and PPh_3 (1 equiv) at 6−10 °C for 8 h. Rh(ttp)Me (1.0 mg, 0.0013 mmol), $H_2{}^{18}O$ (26 μL, 1.3 mmol), and PPh_3 (0.3 mg, 0.0011 mmol) were dissolved in 2,6-dimethylcyclohexanone (500 μL). The reaction mixture was degassed three times by freeze−thaw−pump cycles, purged with N_2, and photolyzed at 6−10 °C under nitrogen for 8 h. 2,6-Dimethylcyclohexanone was collected by vacuum distillation. The crude solution was analyzed by GC/MS, and ^{18}O-enriched 2-heptanone and ^{16}O 2-heptanone were obtained in a 4:1 ratio and added up to a total of 27 turnovers using naphthalene as the internal standard.

Photolysis of 2-Heptanone with Rh(ttp)Me, $H_2{}^{18}O$ (1000 equiv), and PPh_3 (1 equiv) at 6−10 °C for 8 h. Rh(ttp)Me (1.0 mg, 0.0013 mmol), $H_2{}^{18}O$ (26 μL, 1.3 mmol), and PPh_3 (0.3 mg, 0.0011 mmol) were dissolved in 2-heptanone (500 μL). The reaction mixture was degassed three times by freeze−thaw−pump cycles, purged with N_2, and photolyzed at 6−10 °C under nitrogen for 8 h. 2-Heptanone was collected by vacuum distillation. The crude solution was analyzed by GC/MS, and no ^{18}O-enriched 2-heptanone was observed after the labeling reaction.

Thermal Reaction of 2-Heptanone with Rh(ttp)Me, $H_2{}^{18}O$ (1000 equiv), and PPh_3 (1 equiv) at 60 °C for 8 h. Rh(ttp)Me (1.0 mg, 0.0013 mmol), $H_2{}^{18}O$ (26 μL, 1.3 mmol), and PPh_3 (0.3 mg, 0.0011 mmol) were dissolved in 2-heptanone (500 μL). The reaction mixture was degassed three times by freeze−thaw−pump cycles, purged with N_2, and heated to 60 °C under nitrogen for 8 h. 2-Heptanone was collected by vacuum distillation. The crude solution was analyzed by GC/MS, and no ^{18}O-enriched 2-heptanone was observed after the labeling reaction.

Photolysis of 2,6-Dimethylcyclohexanone with $H_2{}^{18}O$ (1000 equiv) and PPh_3 (1 equiv) at 6−10 °C for 8 h. $H_2{}^{18}O$ (26 μL, 1.3 mmol) and PPh_3 (0.3 mg, 0.0011 mmol) were dissolved in 2,6-dimethylcyclohexanone (500 μL). The reaction mixture was degassed three times by freeze−thaw−pump cycles, purged with N_2, and photolyzed at 6−10 °C under nitrogen for 8 h. The crude solution was collected by vacuum distillation and analyzed by GC/MS; 11% of ^{18}O-enriched 2,6-dimethylcyclohexanone was observed after the labeling reaction.

Photolysis of 2,6-Dimethylcyclohexanone with Rh(ttp)Me, D_2O (500 equiv), and PPh_3 (1 equiv) at 6−10 °C for 8 h. Rh(ttp)Me (1.0 mg, 0.0013 mmol), D_2O (13 μL, 0.65 mmol), and PPh_3 (0.3 mg, 0.0011 mmol) were dissolved in 2,6-dimethylcyclohexanone (500 μL). The reaction mixture was degassed three times by freeze−thaw−pump cycles, purged with N_2, and photolyzed at 6−10 °C under nitrogen for 8 h. The crude solution was collected by vacuum distillation and analyzed by GC/MS. 2-Heptanone was obtained in 30 turnovers using naphthalene as the internal standard. Analyzing the crude 2,6-dimethylcyclohexanone revealed it is 8% d_1-enriched after the labeling reaction.

Photolysis of 2,6-Dimethylcyclohexanone with D_2O (1000 equiv) and PPh_3 (1 equiv) at 6−10 °C for 8 h. D_2O (26 μL, 1.3 mmol) and PPh_3 (0.3 mg, 0.0011 mmol) were dissolved in 2,6-dimethylcyclohexanone (500 μL). The reaction mixture was degassed three times by freeze−thaw−pump cycles, purged with N_2, and photolyzed at 6−10 °C under nitrogen for 8 h. 2,6-Dimethylcyclohexanone was collected by vacuum distillation. The crude solution was analyzed by GC/MS, and no d_1-enriched 2,6-dimethylcyclohexanone was observed after the labeling reaction.

Thermal Reaction of Rh(tmp) and 2,6-Dimethylcyclohexanone with D_2O (1000 equiv) and PPh_3 (1 equiv) at 60 °C for 8 h. To a benzene solution of Rh^{II}(tmp) (0.0018 mmol) was added PPh_3 (0.5 mg, 0.0019 mmol), and the reaction mixture was stirred at 25 °C. After 10 min, the benzene solvent was removed by vacuum evaporation and then degassed 2,6-dimethylcyclohexanone (500 μL) and D_2O (35 μL, 1.8 mmol) were added. The mixture was then stirred under nitrogen at 60 °C for 8 h. Excess solvent was collected by vacuum distillation. Rh(tmp)$COCH(CH_3)(CH_2)_3COCH_3$[15] was observed in 72% yield. R_f = 0.08 (hexane/CH_2Cl_2 1/1). ^{1}H NMR (700 MHz, $CDCl_3$): δ −3.29 (sext, 1 H, J = 6.8), −2.23 (d, 3 H, J = 6.7), −1.72 (m, 1 H), −1.40 (m, 1 H), −0.89 (m, 1 H), −0.46 (m, 1 H), 1.20 (m, 2H), 1.63 (s, 3 H), 1.71 (s, 12 H), 2.05 (s, 12 H), 2.61 (s, 12 H), 7.23 (s, 4 H), 7.30 (s, 4 H), 8.54 (s, 8 H). ^{13}C NMR (175 MHz, $CDCl_3$): δ 12.29, 19.43, 29.37, 30.54, 42.82, 49.13, 120.36, 127.95, 130.82, 137.69, 138.43, 139.06, 139.49, 142.81, 206.67 (d, $^1J_{Rh-C}$ = 28.93 Hz), 208.04. HRMS (FABMS): calcd for $[C_{64}H_{65}N_4O_2Rh]^+$ m/z 1025.1377, found m/z 1025.4235. The crude solution was also analyzed by GC/MS, and 5% d_1-enriched 2,6-dimethylcyclohexanone was observed after the labeling reaction.

dx.doi.org/10.1021/om400672t | *Organometallics* 2013, 32, 5391−5401

Reaction of Rh(tmp) and Diisopropyl Ketone with PPh_3 with the Addition of 50 equiv of H_2O at 25 °C for 10 min. To a benzene solution of Rh^{II}(tmp) (0.0089 mmol) was added PPh_3 (2.3 mg, 0.0089 mmol), and the reaction mixture was stirred at 25 °C. After 10 min, the benzene solvent was removed by vacuum evaporation and then degassed diisopropyl ketone (2.0 mL) and H_2O (8 μL) were added. The mixture was then stirred under nitrogen at 25 °C for 10 min. Excess diisopropyl ketone was removed, and the dark red crude product was then purified by column chromatography on silica gel with hexane/CH_2Cl_2 (1/1) as eluent to give a reddish purple solid of Rh(tmp)CO^{i}Pr[15] (7.6 mg, 0.0080 mmol, 90% yield). R_f = 0.52 (hexane/CH_2Cl_2 1/1). ^{1}H NMR (700 MHz, $CDCl_3$): δ −3.33 (hept, 1 H, J = 7.12 Hz), −2.04 (d, 6 H, J = 7.91 Hz), 1.79 (s, 12 H), 1.97 (s, 12 H), 2.61 (s, 12 H), 7.24 (s, 4 H), 7.28 (s, 4 H), 8.53 (s, 8 H). ^{13}C NMR ($CDCl_3$, 175 MHz): 15.46, 43.54, 120.24, 127.83, 130.72, 137.63, 138.49, 139.30, 142.76, 207.05 (d, $^1J_{Rh-C}$ = 32.0 Hz). HRMS (FABMS): calcd for $[C_{60}H_{59}N_4ORh]^+$: m/z 955.0475, found m/z 955.3817. Acetone (76%) was observed in GC/MS using naphthalene as the internal standard. Acetone: t_R = 2.153 min. EIMS: m/z (relative %) 58 (3), 43 (10).

Kinetics Study of the Reaction among Rh(tmp), Diisopropyl Ketone, PPh_3, and Water. *Wavelength Scan.* A UV−visible wavelength scan was carried out on a UV−vis spectrometer equipped with a temperature controller at 25.0 ± 0.2 °C. The temperature of the solution was measured by a Fluke thermometer, with a K-type thermocouple wire placed in an adjacent dummy UV cell filled with benzene inside the sample compartment. The stock benzene solutions of diisopropyl ketone (0.06 mL, 0.0985 M) and Rh(tmp) (0.1 mL, 8.91 × 10^{-4} M) were transferred respectively to the side arm and bottom of a Telfon-stopped Schlenk UV cell with a gastight syringe under N_2 carefully. A stock solution of PPh_3 (0.15 mL, 0.0381 M), H_2O (2 μL), and dried benzene (2.69 mL) were then transferred under N_2 to the same cell using gastight syringe. The solutions were stirred for 10 min at 25.0 ± 0.2 °C inside the sample compartment under N_2. The two stock solutions in the side arm and bottom of the UV cell, respectively, were mixed just before the absorbance was measured. The experimental concentrations were [Rh(tmp)] = 2.97 × 10^{-5} M, [diisopropyl ketone] = 1.97 × 10^{-3} M, [PPh_3] = 1.91 × 10^{-3} M, and [H_2O] = 3.74 × 10^{-3} M at T = 25.0 ± 0.2 °C. Just before the scan, the solutions were mixed by turning the cell upside down. The UV spectra were scanned at 600 nm/min between 350 and 650 nm. The spectra were recorded for 1 h.

Time Scan. A UV−visible time scan was carried out. First, saturation kinetics was done by varying concentrations of PPh_3 (10/30/90/200 μL, 0.038 M) until the rate constant leveled off with increasing concentration. Rh(tmp) (0.075 mL, 8.91 × 10^{-4} M), diisopropyl ketone (0.045 mL, 0.0789 M), and H_2O (2 μL) were added in fixed amounts.

With the optimized concentration of PPh_3, the concentration of Rh(tmp) was then varied. The stock benzene solutions of diisopropyl ketone (0.06 mL, 0.0985 M) and Rh(tmp) (0.1/0.2/0.3/0.4 mL, 4.46 × 10^{-4} M) were carefully transferred separately to the bulb and bottom of a Teflon-stopped Schlenk UV cell with a gastight syringe under N_2. Stock solutions of PPh_3 (0.15 mL, 0.0381 M), H_2O (2 μL) and dried benzene (2.39 - 2.69 mL) were then added under N_2 to the same cell using a gastight syringe to dilute the stock solutions to the desired concentrations. The solutions were stirred for 10 min at 25.0 ± 0.2 °C inside the sample compartment under N_2. The reaction was monitored at 530 nm for 4−5 half-lives.

Then, the concentration of diisopropyl ketone (15/20/25/30/40 μL, 0.118 M) was varied. The dependence of ketone was established by a procedure similar to that shown above, keeping the concentrations of Rh(tmp) (0.1 mL, 4.46 × 10^{-4} M), PPh_3 (0.15 mL, 0.0381 M), and H_2O (2 μL) the same.

Temperature Dependence. Finally, a time scan was carried out at different reaction temperature. The stock benzene solutions of diisopropyl ketone (0.085 mL, 0.0787 M), Rh(tmp) (0.2 mL, 4.46 × 10^{-4} M), PPh_3 (0.15 mL, 0.0381 M) and H_2O (2 μL) were transferred separately to the side arm and bottom of a Teflon-stopped Schlenk UV cell for the reaction. The time scans were repeated at 10.0, 20.0, 30.0, 40.0, and 50.0 ± 0.2 °C, respectively.

■ ASSOCIATED CONTENT

Ⓢ Supporting Information

Figures and text giving details of the $H_2{}^{18}O$ and D_2O labeling experiments, hydrogen detection, calculation and analysis of the kinetic investigation, and GC/MS spectra. This material is available free of charge via the Internet at http://pubs.acs.org.

■ AUTHOR INFORMATION

Corresponding Author

*E-mail for K.S.C.: ksc@cuhk.edu.hk.

Notes

The authors declare no competing financial interest.

■ ACKNOWLEDGMENTS

We thank the Research Grants Council of the HKSAR (No 400309) for financial support.

■ REFERENCES

(1) (a) Goldman, A. S. *Nature* **2010**, *463*, 435−436. (b) Park, Y. J.; Park, J.-W.; Jun, C.-H. *Acc. Chem. Res.* **2008**, *41*, 222−234. (c) Murakami, M.; Makino, M.; Ashida, S.; Matsuda, T. *Bull. Chem. Soc. Jpn.* **2006**, *79*, 1315−1321. (d) Rybtchinski, B.; Milstein, D. *Angew. Chem., Int. Ed.* **1999**, *38*, 870−883. (e) Grochowski, M. R.; Brennessel, W. W.; Jones, W. D. *Organometallics* **2011**, *30*, 5604−5610. (f) Chaplin, A. B.; Green, J. C.; Weller, A. S. *J. Am. Chem. Soc.* **2011**, *133*, 13162−13168.

(2) Murakami, M.; Ito, Y. *Activation of Unreactive Bonds and Organic Synthesis*; Murai, S., Ed.; Springer: Berlin, 1999; Vol. 3, pp 97−98.

(3) (a) Shilov, A. E.; Shul'pin, G. B. *Chem. Rev.* **1997**, *97*, 2879−2932. (b) Crabtree, R. H. *J. Organomet. Chem.* **2004**, *689*, 4083−4091. (c) Bergman, R. G. *Nature* **2007**, *446*, 391−393. (d) Waltz, K. M.; Hartwig, J. F. *Science* **1997**, *277*, 211−213.

(4) Rybtchinski, B.; Vigalok, A.; Ben-David, Y.; Milstein, D. *J. Am. Chem. Soc.* **1996**, *118*, 12406−12415.

(5) Chan, K. S.; Li, X. Z.; Lee, S. Y. *Organometallics* **2010**, *29*, 2850−2856.

(6) Chan, Y. W.; Chan, K. S. *J. Am. Chem. Soc.* **2010**, *132*, 6920−6922.

(7) Lee, S. Y.; Lai, T. H.; Choi, K. S.; Chan, K. S. *Organometallics* **2011**, *30*, 3691−3693.

(8) (a) Matsuda, T.; Makino, M.; Murakami, M. *Org. Lett.* **2004**, *6*, 1257−1259. (b) Murakami, M.; Matsuda, T. *Chem. Commun.* **2011**, *47*, 1100−1105.

(9) Suggs, J. W.; Jun, C.-H. *J. Chem. Soc., Chem. Commun.* **1985**, 92−93.

(10) Jun, C. -H. *Chem. Soc. Rev.* **2004**, *33*, 610−618.

(11) Chatani, N.; Ie, Y.; Kakiuchi, F.; Murai, S. *J. Am. Chem. Soc.* **1999**, *121*, 8645−8646.

(12) Perthuisot, C.; Jones, W. D. *J. Am. Chem. Soc.* **1994**, *116*, 3647−3648.

(13) Liou, S. -Y.; van der Boom, M. E.; Milstein, D. *Chem. Commun.* **1998**, 687−688.

(14) To, C. T.; Choi, K. S.; Chan, K. S. *J. Am. Chem. Soc.* **2012**, *134*, 11388−11391.

(15) (a) Fung, H. S.; Li, B. Z.; Chan, K. S. *Organometallics* **2010**, *29*, 4421−4423. (b) Fung, H. S.; Li, B. Z.; Chan, K. S. *Organometallics* **2012**, *31*, 570−579.

(16) The BDE of the (por)Rh−C bond has been reported: Cui, W.; Wayland, B. B. *J. Am. Chem. Soc.* **2004**, *126*, 8266−8274.

(17) (a) Wayland, B. B.; Sherry, A. E.; Poszmik, G.; Bunn, A. G. *J. Am. Chem. Soc.* **1992**, *114*, 1673−1681. (b) Sherry, A. E.; Wayland, B. B. *J. Am. Chem. Soc.* **1989**, *111*, 5010−5012.

(18) Kadish, K. M., Smith, K. M., Guilard, R., Eds. *The Porphyrin Handbook*; Academic Press: Boston, 2000; Vol. *14*.

(19) McLendon, G.; Miller, D. S. *J. Chem. Soc., Chem. Commun.* **1980**, 533−534.
(20) (a) Irie, R.; Li, X.; Saito, Y. *J. Mol. Catal.* **1983**, *18*, 263−265. (b) Irie, R.; Li, X.; Saito, Y. *J. Mol. Catal.* **1984**, *23*, 17−22. (c) Irie, R.; Li, X.; Saito, Y. *J. Mol. Catal.* **1984**, *23*, 23−27.
(21) (a) Behar, D.; Dhanasekaran, T.; Neta, P.; Hosten, C. M.; Ejeh, D.; Hambright, P.; Fujita, E. *J. Phys. Chem. A* **1998**, *102*, 2870−2877. (b) Morris, A. J.; Meyer, G. J.; Fujita, E. *Acc. Chem. Res.* **2009**, *42*, 1983−1994.
(22) Silva, E.; Pereira, M. M.; Burrows, H. D.; Azenha, M. E.; Sarakha, M.; Bolte, M. *Photochem. Photobiol. Sci.* **2004**, *3*, 200−204.
(23) Chen, H.; An, T.; Fang, Y.; Zhu, K. *J. Mol. Catal. A: Chem.* **1999**, *147*, 165−172.
(24) Yu, M.; Fu, X. *J. Am. Chem. Soc.* **2011**, *133*, 15926−15929.
(25) (a) Inoue, H.; Sumitani, M.; Sekita, A.; Hida, M. *J. Chem. Soc., Chem. Commun.* **1987**, 1681−1682. (b) Funyu, S.; Kinai, M.; Masui, D.; Takagi, S.; Shimada, T.; Tachibana, H.; Inoue, H. *Photochem. Photobiol. Sci.* **2010**, *9*, 931−936.
(26) Fukuzumi, S.; Kishi, T.; Kotani, H.; Lee, Y. M.; Nam, W. *Nat. Chem.* **2011**, *3*, 38−41.
(27) (a) Kalita, D.; Radaram, B.; Brooks, B.; Kannam, P. P.; Zhao, X. *ChemCatChem* **2011**, *3*, 571−573. (b) Singh, W. M.; Pegram, D.; Duan, H.; Kalita, D.; Simone, P.; Emmert, G. L.; Zhao, X. *Angew. Chem., Int. Ed.* **2012**, *51*, 1653−1656.
(28) (a) Chen, W.; Rein, F. N.; Rocha, R. C. *Angew. Chem.* **2009**, *121*, 9852−9855; *Angew. Chem., Int. Ed.* **2009**, *48*, 9672−9675. (b) Chen, W.; Rein, F. N.; Scott, B. L.; Rocha, R. C. *Chem. Eur. J.* **2011**, *17*, 5595−5604.
(29) Li, F.; Yu, M.; Jiang, Y.; Huang, F.; Li, Y.; Zhang, B.; Sun, L. *Chem. Commun.* **2011**, *47*, 8949−8951.
(30) (a) Hamelin, O.; Guillo, P.; Loiseau, F.; Boissonnet, M. -F.; Ménage, S. *Inorg. Chem.* **2011**, *50*, 7952−7954. (b) Guillo, P.; Hamelin, O.; Batat, P.; Jonusauskas, G.; McClenaghan, N. D.; Ménage, S. *Inorg. Chem.* **2012**, *51*, 2222−2230.
(31) Wayland et al. reported that the BDE of Rh^{III}(tmp)−OMe is 46 kcal mol^{-1}. The BDE of the Rh^{III}(ttp)−OH bond is assumed to be similar in strength. See: Sarkar, S.; Li, S.; Wayland, B. B. *J. Am. Chem. Soc.* **2010**, *132*, 13569−13571.
(32) Choi, K. S.; Lai, T. H.; Lee, S. Y.; Chan, K. S. *Organometallics* **2011**, *30*, 2633−2635.
(33) The reaction of Rh(tmps) with H_2O has been reported to generate Rh(tmps)OH (tmps = tetrakis(3,5-disulfonatomesityl) porphyrin); see: Li, S.; Wayland, B. B. *Inorg. Chem.* **2006**, *45*, 9884−9889.
(34) March, J. *Advanced Organic Chemistry: Reactions, Mechanisms, and Structure*, 4th ed.; Wiley-Interscience: New York, 1992; p 243.
(35) Luo, Y. R. *Comprehensive Handbook of Chemical Bond Energies*; CRC Press: Boca Raton, FL, 2007.
(36) Lide, D. R. *Handbook of Chemistry and Physics*, 85th ed.; CRC Press: Boca Raton, FL, 2005.
(37) The decarbonylation rate constant of the acyl radical is at least 10^4 s^{-1} except for the PhCO radical: Garcia-Garibay, , M. A.; Campos, , L. M. In *Handbook of Organic Photochemistry and Photobiology*; Horspool, , W. M., Lenci, , F., Eds.; CRC Press: Boca Raton, FL, **2004**,; Vols. *1*, and *2*,, Chapter 48.
(38) (a) Ogoshi, H.; Setsune, J.; Omura, T.; Yoshida, Z. *J. Am. Chem. Soc.* **1975**, *97*, 6461. (b) Wayland, B. B.; Sherry, A. E.; Poszmik, G.; Bunn, A. G. *J. Am. Chem. Soc.* **1992**, *114*, 1673−1681.
(39) (a) Collman, J. P.; Boulvtov, R. *J. Am. Chem. Soc.* **2000**, *122*, 11812−11821. (b) Wayland, B. B.; Sherry, A. E.; Bunn, A. G. *J. Am. Chem. Soc.* **1993**, *115*, 7675−7684.
(40) Hydroxide ion from H_2O involved in the oxidation of alcohol has been demonstrated: (a) Zope, B. N.; Hibbitts, D. D.; Neurock, M.; Davis, R. J. *Science* **2010**, *330*, 74−78. (b) Balaraman, E.; Khaskin, E.; Leitus, G.; Milstein, D. *Nat. Chem.* **2013**, *5*, 122−125.
(41) *I* strain in a six-membered cyclic ketone explained the high reactivity of cyclohexanone toward a carbonyl reagent; see: Brown, H. C.; Fletcher, R. S.; Johannesen, R. B. *J. Am. Chem. Soc.* **1951**, *73*, 212−221.
(42) Treadway, J. A.; Moss, J. A.; Meyer, T. J. *Inorg. Chem.* **1999**, *38*, 4386−4387.
(43) For literature methods to generate Rh_2(ttp)$_2$ from Rh(ttp)H, see: (a) Collman, J. P. L.; Barnes, C. E.; Woo, L. K. *Proc. Natl. Acad. Sci. U.S.A.* **1983**, *80*, 7684. (b) Wayland, B. B.; Van Voorhees, S. L.; Wilker, C. *Inorg. Chem.* **1986**, *25*, 4039−4042.
(44) Mak, K. W.; Chan, K. S. *J. Am. Chem. Soc.* **1998**, *120*, 9686−9687.
(45) Huck, L. A.; Wan, P. *Org. Lett.* **2004**, *6*, 1797−1799.
(46) Fu, X.; Li, S.; Wayland, B. B. *J. Am. Chem. Soc.* **2006**, *128*, 8947−8954.
(47) For a detailed description of the proposed kinetic scheme, see page S5 in the Supporting Information.
(48) The generation of H_2 from dehydrogenation of Rh(ttp)H in the stoichiometric thermal reaction does not operate according to the reasoning proposed in the main text of this report.
(49) Del Rossi, K. J.; Zhang, X. X.; Wayland, B. B. *J. Organomet. Chem.* **1995**, *504*, 47−56.
(50) Yang, C.-H.; Dazugan, S. J.; Goedken, V. L. *J. Chem. Soc., Chem. Commun.* **1985**, 1425−1426.
(51) Wang, J. C.; Xu, Z. J.; Guo, Z.; Deng, Q. H.; Zhou, C. Y.; Wan, X. L.; Che, C. M. *Chem. Commun.* **2012**, *48*, 4299−4301.
(52) Arkady, B. J.; Ellern, A.; Woo, K. *Organometallics* **2012**, *31*, 3628−3635.
(53) Brand, H.; Arnold, J. *Coord. Chem. Rev.* **1995**, *140*, 137−168.
(54) The estimation of the (tmp)Rh−OH bond length is based on the report on (tmcp)Rh(H_2O) (tmcp = tetramethylchiroporphyrinato dianion): Simonato, J.-P.; Pécaut, J.; Marchon, J. -C. *Inorg. Chim. Acta* **2001**, *315*, 240−244.
(55) (a) Wagner, R. W.; Lawrence, D. S.; Lindsey, J. S. *Tetrahedron Lett.* **1987**, *28*, 3069−3070. (b) Chan, K. S.; Chen, X. M.; Mak, T. C. W. *Polyhedron* **1992**, *11*, 2703−2716.
(56) (a) Zhou, X.; Li, Q.; Mak, T. C. W.; Chan, K. S. *Inorg. Chim. Acta* **1998**, *270*, 551−554. (b) Zhou, X.; Wang, R.-J.; Xue, F.; Mak, T. C. W.; Chan, K. S. *J. Organomet. Chem.* **1999**, *580*, 22−25.
(57) Wayland, B. B.; Sherry, A. E.; Poszmik, G.; Bunn, A. G. *J. Am. Chem. Soc.* **1992**, *114*, 1673−1681.
(58) Gol'dshleger, N. F.; Tyabin, M. B.; Shilov, A. E.; Shteinman, A. A. *Russ. J. Phys. Chem.* **1969**, *43*, 1222.